DEVELOPMENT OF A MULTI-STATE FLUIDLASTIC® LEAD-LAG DAMPER

Conor Marr
Senior Engineer
LORD Corporation
conor.marr@lord.com

Haris Halilovic
Engineering Manager
LORD Corporation
haris.halilovic@lord.com

LORD Corporation
Mechanical Technology
Erie, PA
U.S.A

ABSTRACT

Building onto extensive damper knowledge and experience LORD has designed and is validating a passive multi-state Fluidlastic® lead-lag damper to reduce damper forces when high damping is not required. This variable damping was achieved via a set of bypass features that are opened or closed by the changing centrifugal force associated with the rotor speed. A first generation prototype was fabricated with an internal sliding spring/mass system to open or close a set of bypass channels with varying rotor speed. Bench testing of the first generation prototype demonstrated a large reduction in damping with the bypass channels open, and spin testing validated the CF actuation concept. A second generation damper was designed to integrate the bypass feature into the piston, resulting in a multi-state device that has the same space envelope with negligible impact on damper weight. The second generation damper was bench tested to validate a 50% damping reduction. The integrated CF actuation system was proven via spin tests. Additionally, ANSYS CFX® was used to create a detailed computational fluid dynamics (CFD) model to predict the damper behavior. The CFD model accurately predicts damper forces in the closed configuration with an average error in peak force prediction of approximately 5% and an average error in loss stiffness prediction of less than 10%. The CFD model predicts damper forces in the open configuration, with an average peak force error approaching 5%. Prediction errors of the loss stiffness for the open case are close to 10%.

1. INTRODUCTION

Lead-lag dampers are a critical component in most rotorcraft systems, providing high damping at low rotor speeds to prevent destructive ground resonance instabilities and enough damping during flight to eliminate uncomfortable blade oscillations. Though high damping is needed to eliminate these instabilities only over a small region of the helicopter's operating conditions, the conventional damper continues to produce high damping in all conditions, leading to high root end loads and reduced component life. In forward flight especially, the 1/rev frequency blade motion generates high forces across the lead-lag damper. LORD Corporation has been a leader in developing new damper technologies over the past five decades, continuously investigating new concepts to further improve damper performance. A simple passive multi-state bypass damper is currently being developed to help reduce high blade root loads associated with the use of conventional lead-lag dampers and to further improve damper reliability.

1.1 History of Lead-Lag Damper Development

There are three types of conventional lead-lag dampers that are currently in use: hydraulic, elastomeric, and Fluidlastic®. Used in a variety of configurations, from the most common blade to hub attachment to more unique inter-blade dampers, each of the three types has benefits that keep them in use on a variety of rotorcraft.

Replacing the unreliable friction dampers of early rotorcraft designs, the hydraulic orifice damper was introduced in the 1960s and is still widely used today [1]. Hydraulic lag dampers work by forcing a viscous fluid through restrictive orifices and valves, creating both a pressure drop across a piston head and viscous losses that provide damping to the blade lag motion [2]. Similar to an idealized dashpot, simple hydraulic dampers provide damping energy losses proportional to the square of the lag speed, though more complex internal geometry can alter this behavior [1].

Despite being an older concept, hydraulic dampers are still in use on most larger helicopters because they can provide more damping than some of the newer damper types [3]. The Sikorsky UH-60 Blackhawk and the Boeing CH-47 Chinook are two examples of rotorcraft still using hydraulic dampers for this reason [2]. Though hydraulic dampers provide high damping and are widely used, they have many drawbacks. Due to their reliance on a complex set of fluids, seals, and lubricants, all subjected to the adverse rotor environment of high centrifugal and dynamic loads, the hydraulic damper requires high maintenance. A minor defect, such as a leak, can be very harmful to the damper's performance [4]. The highly viscous fluids themselves can be dangerous to both operators and the environment in the event of a leak, further increasing the importance of proper maintenance [2]. Additionally, foreign objects such as dirt and sand can greatly reduce the damper's performance and life if they come in contact with the lubrication and seals.

LORD Corporation developed the elastomeric damper to solve some of the issues with the hydraulic damper. Elastomeric dampers use dynamic shearing of their elastomeric layers to dissipate energy, eliminating the need for a fluid-filled device [4]. Additionally, the elastomer has an inherent stiffness, thus providing both damping and stiffness to the rotor system [1]. Unlike hydraulic dampers, elastomeric dampers are generally unaffected by sand and dust because there are no sliding interfaces [2]. Where hydraulic dampers can be difficult to inspect due to their many internal components, elastomeric dampers have a gradual degradation modes that can be readily observed with a simple visual inspection [4]. Elastomeric dampers have proven to be very reliable and are in use on, for example, the Boeing AH-64 Apache, the MD500 and many other helicopter platforms [2].

Despite their many benefits, elastomeric dampers are not able to provide enough damping to make them suitable for large scale helicopters such as the UH-60 and the CH-53. Their performance also depends heavily on dynamic strain, frequency, and temperature. Designing one for the whole flight envelope is somewhat complicated [1]. Lastly, since they are mechanically simple with no sliding parts, the ability to tailor their behavior can be limited.

LORD Corporation introduced the Fluidlastic® damper technology to combine the benefits of both the elastomeric and hydraulic damper. The Fluidlastic® damper technology, in its basic concept, is a fluid-elastic device, embedding fluid chambers within an elastomeric housing [2]. The dynamic shearing of the elastomeric damper and the viscous energy dissipation of the hydraulic damper combine to create the damping force. Similar to many hydraulic dampers, some Fluidlastic® dampers contain volume compensators that control pressure changes in the fluid due to thermal expansion and contraction, thus minimizing temperature effects on the dynamic characteristics of the damper [3]. Additional design degrees of freedom permit the performance of fluid-elastic dampers to be easily tailored.

Since Fluidlastic® dampers combine the hydraulic pumping of fluid with elastomeric straining, they are able to provide significant damping forces, making them ideal replacements for hydraulic dampers. The elastomeric housing hermetically seals the damper, eliminating the need for moving seals and greatly reducing the effects of sand and dust, leakage, and maintenance time [3].

1.2 Previous Adaptable Damper Designs

The concept of a multi-state or frequency selective damper has been around for decades, though many of the designs that are currently in use in the automotive and civil industries do not translate well into the rotorcraft environment [5-6]. Work has been done on bypass dampers in the past, proving the merit of the concept, though current designs require an active controller to change between damper states [7].

Magnetorheological (MR) and Electrorheological (ER) dampers are semi-active damping devices that use varying magnetic or electrical fields respectively to change the resistance of the damper. These semi-active devices can be found in varying systems from suspension systems and engine mounts, to structural dampers to counteract earthquake and wind loadings [8, 9]. Many studies have looked into using MR and ER fluids with a bypass channel that contains an adjustable magnetic or electric field to create a semi-active or adjustable state damping device [5, 10-12].

A comparison of the behavior of an experimental MR damper to the linearized complex modulus model of the damper developed by Wereley and Pang can be seen in **Figure 1** [8]. The effect of the strong centrifugal force in the rotor environment on the suspended particles needs to be considered when using MR and ER technology in lead-lag dampers.

Though MR and ER fluids are a fairly hot topic in the adaptable damper community, there have been a variety of other methods of achieving multi-state devices. Petrie and Wang both attempted to use the out of phase motion of the internal fluid at the lag/rev frequency in an embedded fluid elastic device to provide lead-lag damping [13,14]. Unfortunately, multi-state dampers which depend on out of phase fluid movement do not work well for articulated rotors since higher frequencies are required to produce adequate damping. More research needs to be done into the multi-state behavior of the out of phase device to determine how much of a reduction in damping force can be achieved [14].

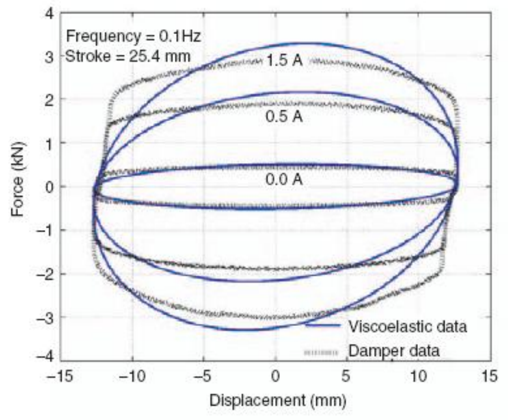

Figure 1: Linearized Complex Model Compared to Experimental MR Damper [5]

Additional frequency dependent devices, such as Reeds frequency selective hydraulic damper for rotorcraft are generally complicated mechanical systems that have little to no experimental or analytical validation [6].

1.3 Bypass Dampers

The automotive community has been using multi-state bypass dampers for many years, such as the experimental two-state car suspension system developed by Tavner, *et al*. [15]. Bottasso *et al*. began an investigation into the effects of applying a multi-state bypass damper to the rotorcraft environment. They proposed a semi-active damper that changes the state of a bypass valve with varying flight condition [7]. A mathematical model was made and tuned with experimental data to match a mono-tube hydraulic damper with pressure relief valves and a bypass channel, and then coupled with a multi-body model of the A109E helicopter [7]. The resulting predicted decrease in damper load with varying blade azimuth is highlighted in **Figure 2**. In addition to the semi-active flight regime control, a higher harmonic control system was integrated into the rotor simulation that opened and closed the bypass valve to reduce harmonic amplitudes [7]. The predictions clearly demonstrate the theoretical decrease in forces that a semi-active bypass damper can produce. In situations where full feedback control is not needed, a passive system can offer targeted multi-state behavior. Initial work on a multi-phase passive damper was done by Marr *et. al.* [16].

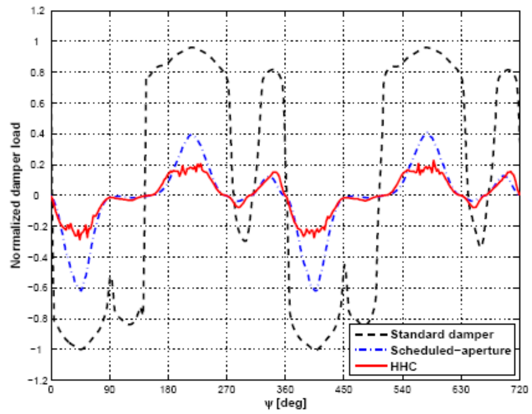

Figure 2: Multi-State Damper Load vs. Blade Azimuth [7]

2. OBJECTIVES

The objectives of this research are to design, construct, and experimentally validate a passive or semi-active LORD Fluidlastic® bypass damper that greatly reduces damper forces when damping is not required. These objectives are broken into four main tasks:

1) Design and construct a first and second generation LORD Fluidlastic® bypass damper prototype that can meet the damping requirements at the lead-lag frequency for a generic light/medium helicopter while reducing damper force by at least 50% at the nominal rotor frequency (1/rev) via a bypass feature that will open when high damping is not required.
2) Conduct a series of experimental bench tests to evaluate the performance of the two prototype dampers with bypass features open and closed.
3) Develop CFD models of the bypass damper prototypes and use the models to predict the damper behavior at key frequencies and displacements. Validate with experimental data.
4) Spin test bypass damper prototypes to validate the CF actuation concepts for both the first and second generation prototypes.

3. MULTI-STATE DAMPER DESIGN

The basic concept of a bypass damper is fairly straight forward, but requires some form of actuation to make it into a multi-state device. While these dampers have been used with much success in other realms, the complex rotating environment of the rotor system creates many issues with current designs. Additionally, the incorporation of a device that requires both power and some sort of sensing or communication with the flight computer is less than ideal, requiring the use of a complicated slip ring. A passive or semi-passive device would make the device much more attractive to the rotorcraft community.

Articulated rotors normally encounter the ground resonance instability region between 0.2/rev and 0.4/rev. As such, the danger region is between 20% and 40% of the nominal main rotor RPM. An example Coleman diagram is shown in **Figure 3**, highlighting the regions of instability for a rotor system with a nominal rotor speed of 350 RPM and a lag frequency at 0.4/rev corresponding to 140 RPM. Soft and stiff-in-plane rotors generally avoid the ground resonance phenomena, but may require lag damping to eliminate air resonance or during heavy maneuvering flight. A passive bypass damper that can be in a closed state during the regions requiring high damping, but an open bypass feature state during nominal flight would greatly reduce the loads seen by the damper and the hub and blade attachment points.

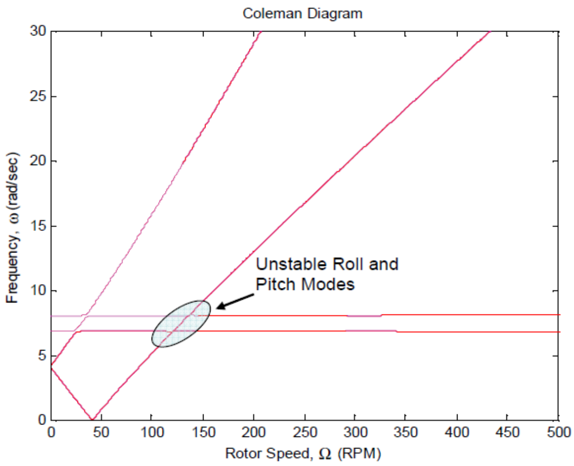

Figure 3: Example Coleman Diagram Showing Instability Regions

Based on the previously stated requirements, a conceptual LORD Fluidlastic® multi-state damper was designed. The basic premise involves modifying a LORD Fluidlastic® damper by adding bypass features. When in the closed state, the bypass features are blocked by a control valve and all of the highly viscous fluid is forced across the piston, creating high damping. In the open state, the fluid bypasses the restrictive flow features, greatly reducing the damper force. The number and size of the bypass features allows the decrease in damping force to be tailored to the desired behavior, while alteration of the piston size, orifice number and size, and fluid properties all allow the specific damping properties of the device to be selected.

The first generation prototype has a set of external bypass channels and a sliding ring mass to demonstrate the CF activation and reduction in damping. **Figure 4** shows a cross sectional view of the first generation prototype.

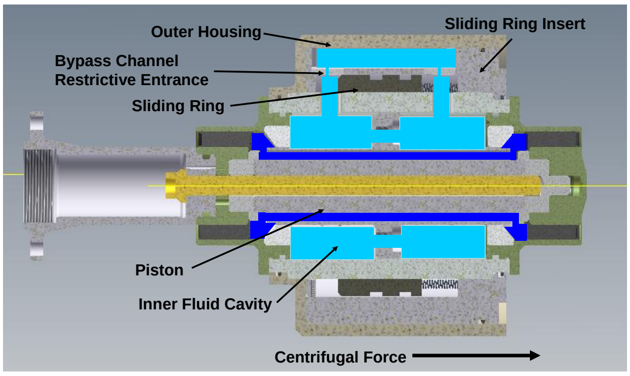

Figure 4: First Generation CF Damper Prototype

The second generation prototype integrates the CF actuated sliding mass into the piston head, as seen in the piston cross sectional view of the second generation prototype in **Figure 5**. This configuration enables the damper to have multi-state behavior without altering the original damper space envelope and with a negligible effect on weight.

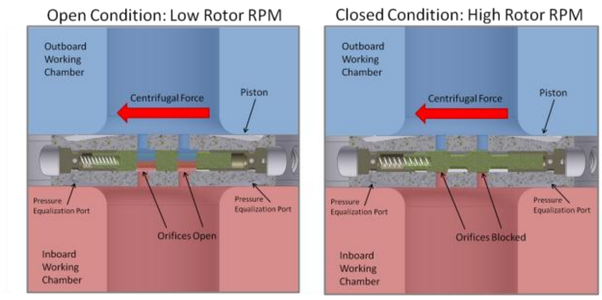

Figure 5: Second Generation CF Damper Prototype

3.1 CFD Approach

Advances in the past decade have greatly improved the accuracy of computational fluid dynamics (CFD) programs. The incorporation of moving/deforming meshes, more detailed fluid properties, and detailed turbulence and separation models have added to this accuracy. Additionally, CFD acts like a sensor anywhere within the flow stream, allowing visualization of many aspects of the flow, including velocity, pressure fields, vorticity, and the ability to track individual fluid particles.

For this study, ANSYS CFX was used to predict the damper behavior. Four models were developed to predict the damper behavior. The first two models capture the open and closed behavior of the first generation prototype. The second two models capture the open and closed behavior of the second generation prototype.

Each model was developed to mirror the behavior of the experimental tests and capture the exact conditions that each damper would undergo. As such, a dynamic meshing model was constructed, allowing the piston to move within the damper housing just as it would in the real part, greatly increasing the accuracy of the models. A cross section of the mesh of the first generation damper interior with a 0.1 inch bypass pipe is pictured in **Figure 6.**

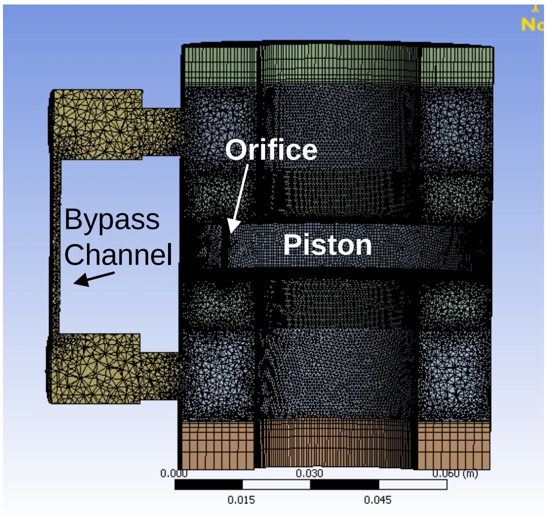

Figure 6: CFD Mesh Cross Section

3.2 Bench Test Experiments

In order to conduct experimental bench tests, two prototypes were designed and constructed to meet the generic light/medium helicopter requirements. Each device includes embedded bypass features that can be set to an open or closed state during assembly. Both devices were designed to be highly customizable with alterable flow feature geometries and fluid properties. The key device parameters for the first generation design are listed in Table 1.

Table 1. Key Prototype Parameters

Parameter	English	Metric
Piston Diameter	2.74 in	70 mm
Bypass Diameter	3 x 0.4 in	3 x 1 mm

Following the construction and assembly of the first generation damper, a series of tests were conducted on a hydraulic single-axis test stand. The test stand generates input displacement amplitude over a range of frequencies, measuring the resistive force generated by the damping device to the input. For the initial test, a series of three frequencies and four dynamic displacements were chosen for the test matrix. The damper was run at 0.04, 0.06, 0.08, and 0.1 inch dynamic displacements at frequencies of 2.5 Hz, 4 Hz, and 6 Hz. Additionally, a semi-static flexing of the damper was conducted to determine the static stiffness of the part. During each case, the force versus displacement data was collected. A photograph of the first generation prototype installed in the hydraulic since-axis test stand can be seen in **Figure 7**.

Figure 7: Damper Prototype in Test Stand

3.3 Spin Test Experiments

After proving the bypass behavior in the best tests, both prototype dampers were then tested in the rotating environment to validate the CF actuation of the bypass features. The spin tests were conducted on The Pennsylvania State University Adverse Environment Rotor Test Stand (AERTS). A dynamic testing apparatus was constructed to test the damping reduction during varying rotor conditions for the first prototype. A photograph of the first generation prototype installed in AERTS facility can be seen in **Figure 8**. The second generation prototype was spin tested with sensors embedded in the bypass features to monitor the opening and closing behavior due to the varying CF.

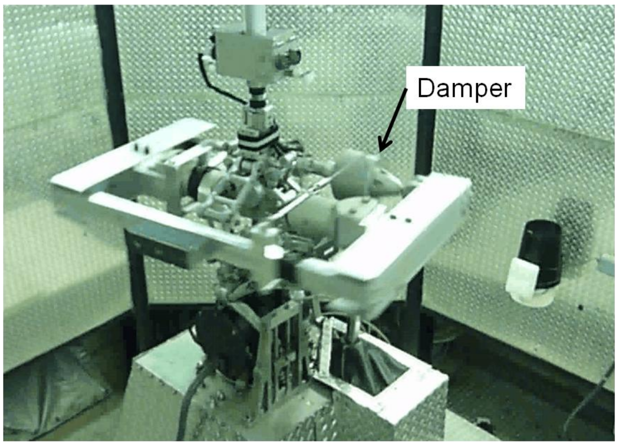

Figure 8: AERTS Spin Test

4. RESULTS

4.1 CFD Prediction

An example of the flow visualization for the damper with bypass channels closed can be seen in **Figure 9** in the form of velocity vectors. This is a cross sectional view of the first generation prototype, which has three bypass channels and one restrictive orifice. The solid piston is marked by the white area in the middle of the CFD model cross section. At this instant in time, the piston is moving downwards, forcing flow up through the restrictive orifice. The high speed exit plume from the orifice can be seen.

To highlight the flow changes captured by CFD the same instant in time at the same cross section of the damper for various bypass channel diameters is shown **Figures 9 through 11**. Each figure has the velocity vectors set to the same scale as the closed bypass channels case in **Figure 9**. As the diameter of the bypass channels increase, the majority of the flow migrates from the restrictive orifice to the bypass channels. At a bypass channel of approximately 0.15 inches in diameter, the flow speed through the bypass channels and the orifice are nearly the same. After this point, the majority of the flow quickly transfers to the bypass channels until the 0.4 inch diameter case where nearly 95% of the flow is through the bypass channels. Comparison of the figures shows how the increasing bypass channels greatly reduce the overall flow speed within the damper, which corresponds to a decrease in the damper force.

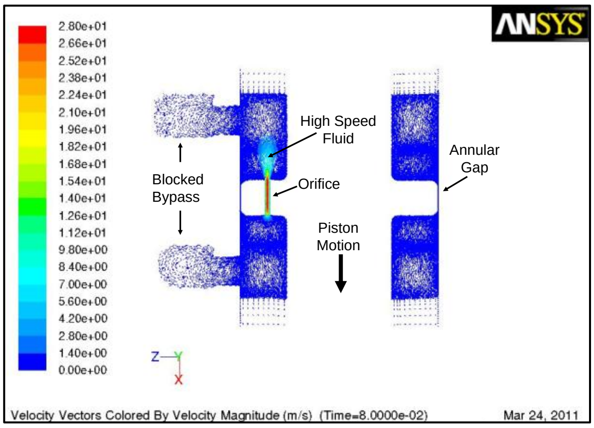

Figure 9: CFD Velocity Vectors with Closed Bypass, Flow Prominently Through the Orifice

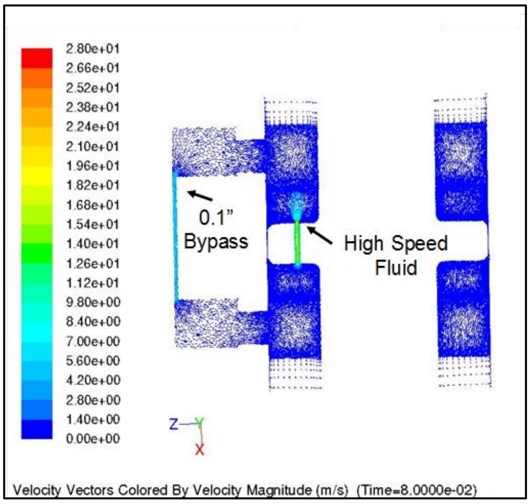

Figure 10: Velocity Vectors, 0.1" Diameter Bypass, Orifice Flow Still Prominent

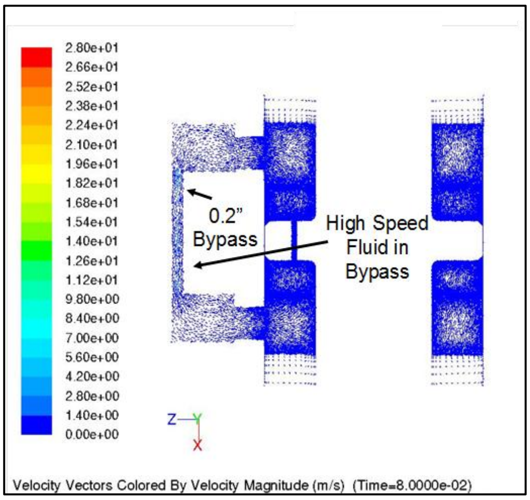

Figure 11: Velocity Vectors, 0.2" Diameter Bypass, Bypass Flow Now Prominent

The force vs. displacement behavior of the damper with five different bypass channel diameters is shown in **Figure 12**. There is an exponential increase in damper force with decreasing bypass diameter, which corresponds to the decreasing overall flow speed seen in the previous CFD case cross sections. This can be seen even more clearly in **Figure 13**, which plots the damper force for each of the damper diameters at one of four time steps. There is a knee in the predicted force behavior around a bypass channel of 0.15 inches in diameter, with a marked increase in damper forces for smaller diameters. Again, this corresponds to flow patterns seen in the CFD cases, with the knee occurring right where the flow speeds through the orifice and bypass channels are near equal.

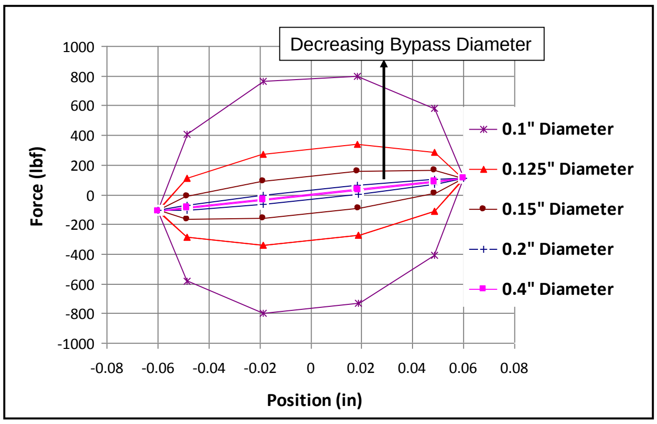

Figure 12: CFD Prediction of Various Bypass Channels

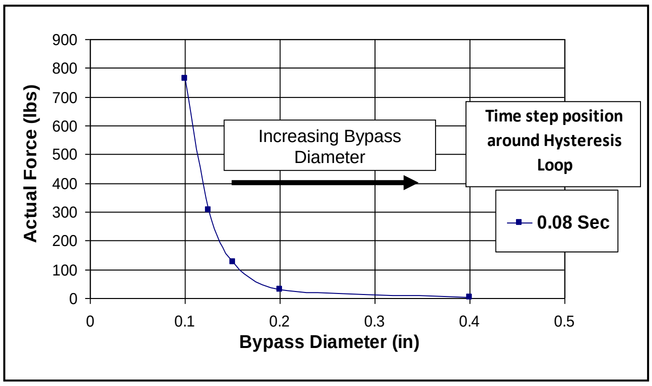

Figure 13: CFD Bypass Effect

A more detailed analysis was conducted during the design of the second generation prototype. After building confidence in the CFD prediction capabilities while modeling the first generation prototype, CFD was used in the design of the second generation damper bypass orifices. **Figure 14** shows an example pressure drop across the piston when the bypass orifice is blocked and in the closed position. **Figure 15** shows the same case, but with the bypass orifice in the open configuration.

The flow is now split between the main orifice and the secondary CF actuated orifice, providing approximately a 50% reduction in damper force. **Figure 16** shows a close up of the flow behavior for this open condition.

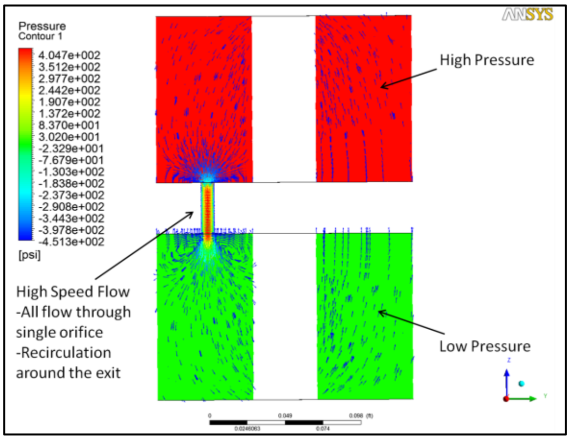

Figure 14: Second Generation Prototype, Bypass Orifice Closed

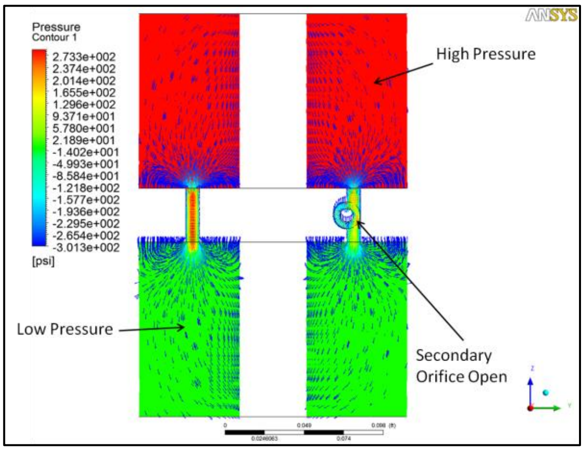

Figure 15: Second Generation Prototype, Bypass Orifice Open

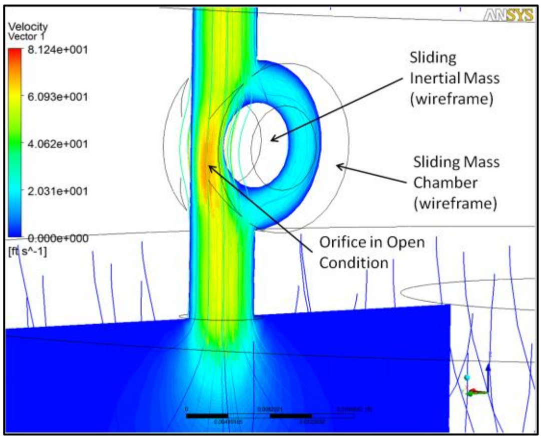

Figure 16: Second Generation Prototype, Close-Up of Open Bypass Orifice

4.2 Bench Test Results, First Generation

Concurrently with the CFD model development and runs, the first generation experimental damper prototype was constructed and tested. The first bench test was a frequency and dynamic displacement sweep to characterize the damper in the closed configuration. For the generic light/medium helicopter configuration, the important frequencies are the blade lag frequency of 2.5 Hz and the 1/rev frequency of 6 Hz.

The force vs. displacement hysteresis loops of these two frequencies for the first generation prototype undergoing the 0.06 inch displacement case can be seen in **Figure 17**. As expected, there is an increase in damping with increasing stroke frequency.

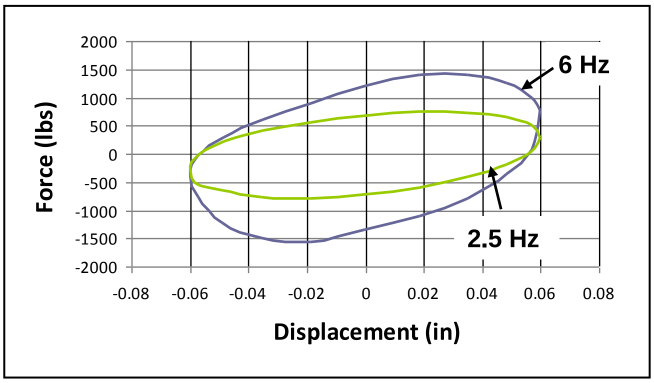

Figure 17: Experimental Data, Bypass Channels Closed

Figures 18 and 19 show experimental storage and loss stiffness respectively. These values were calculated for each frequency and dynamic displacement test condition based on the time history data. The increasing stiffness of the part with increasing frequency can be seen in **Figure 18**, while the increased damping due to frequency can be seen in **Figure 19**. The effect of dynamic displacement on both the stiffness and damping varies with frequency as well.

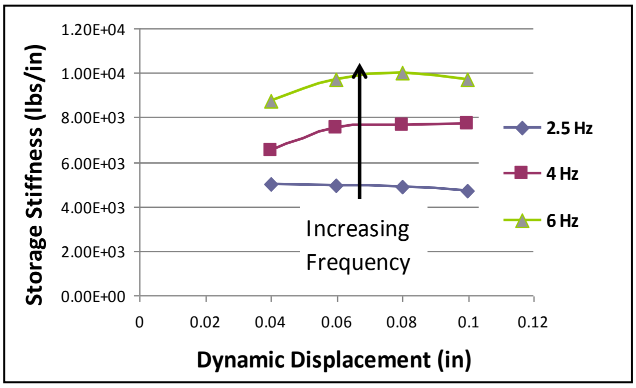

Figure 18: Experimental Storage Stiffness, No Bypass

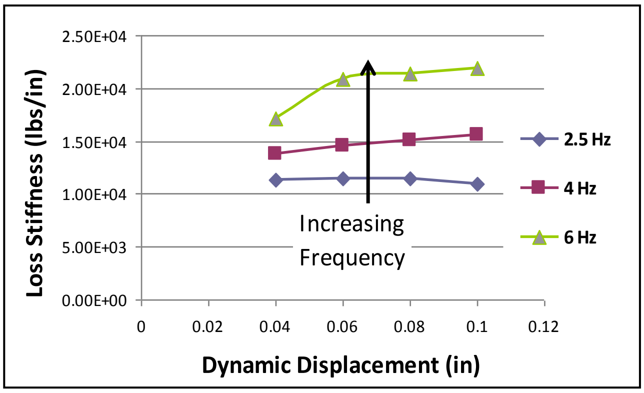

Figure 19: Experimental Loss Stiffness, No Bypass

After characterizing the closed damper, the same set of conditions was run for the damper with the bypass channels in the open configuration. The initial testing used bypass channels with a diameter of 0.4 inches. **Figures 20 and 21** highlight the reduction in damping when the bypass channels are open for the 2.5 Hz case with a dynamic displacement of 0.06 inches and the 6 Hz case with a dynamic displacement of 0.06 inches respectively. For both cases, the peak forces are reduced by approximately 70%, while the damping is reduced by close to 80% with a large component of the force in the open configuration coming from the damper elastomer portions.

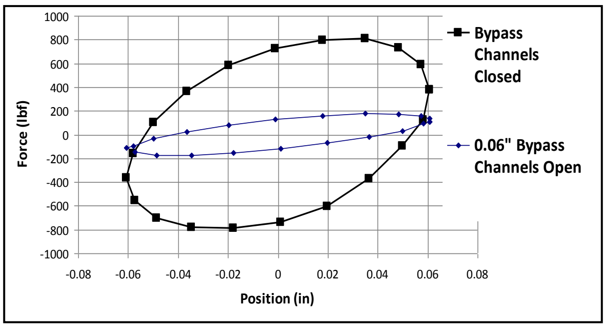

Figure 20: Experimental Data, Bypass Effect at 2.5 Hz

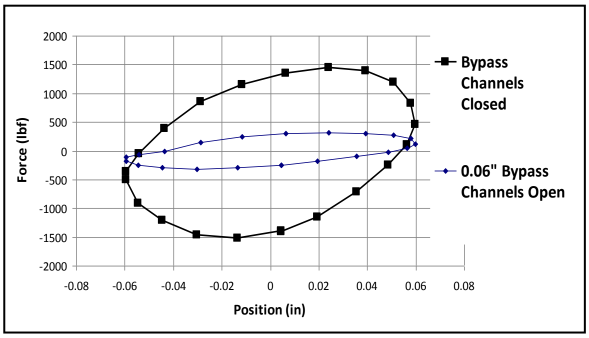

Figure 21: Experimental Data, Bypass Effect at 6 Hz

Since this was the first generation prototype, the larger than desired damping was deemed acceptable since the concept was proven. The second generation damper was designed to achieve the target of the 50% reduction in damping.

A comparison of the reduction of the loss stiffness further demonstrates the effectiveness of the bypass channels. **Figure 22** shows the loss stiffness over the range of experimental cases. There is an average reduction in loss stiffness of over 80%, as can be seen clearly in the figures. Again, the stiffness and damping come almost exclusively from the elastomer end caps.

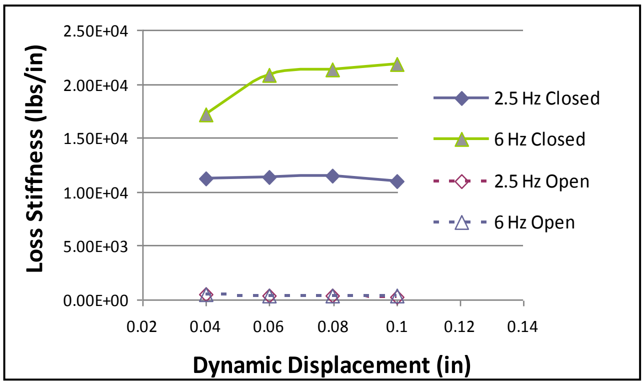

Figure 22: Experimental Loss Stiffness, Bypass Effect

4.3 Bench Test Results and CFD Comparison, Second Generation

Bench testing of the second generation prototype demonstrated the effectiveness of the integrated CF actuation concept. **Figure 23** shows that there is approximately 50% reduction in damping force for the forward flight condition between the opened and closed states. The hysteresis loop data for this case has been normalized to the maximum positive force of the closed case.

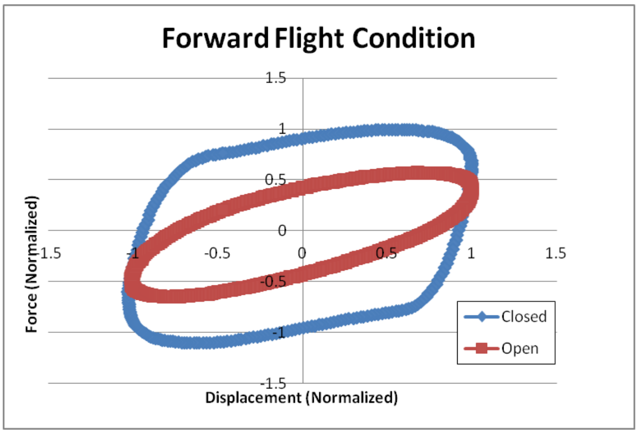

Figure 23: Normalized Second Generation Forward Flight Case, Open and Closed Bypass Orifices

The CFD results were then compared with the experimental bench test results. **Figure 24** compares both the open and closed conditions for the ground resonance condition, where approximately a 50% reduction was predicted and achieved. The results for this hysteresis loop are normalized to the maximum positive force achieved by the experimental case in the closed condition. The force predictions were off by under 5% while the loss stiffness predictions were off by under 10%.

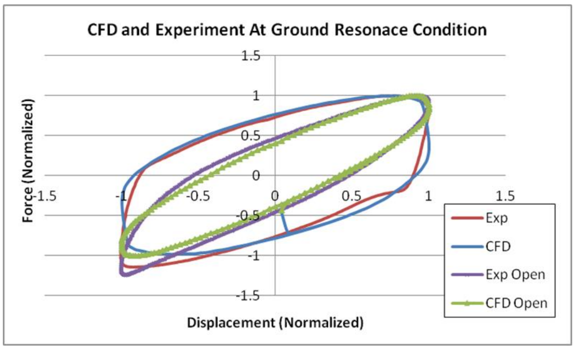

Figure 24: Test vs. CFD Comparison

4.4 Spin Test Results

Following the successful bench testing of the first generation prototype, the damper was tested in the rotating environment. **Figure 25** compares the force vs. time history of the first generation prototype being dynamically actuated in the rotating environment over a range of rotor speeds. High damping is maintained through the ground resonance rotor speed region of 140 RPM, and then decreases by approximately 50% by the time full rotor speed is achieved.

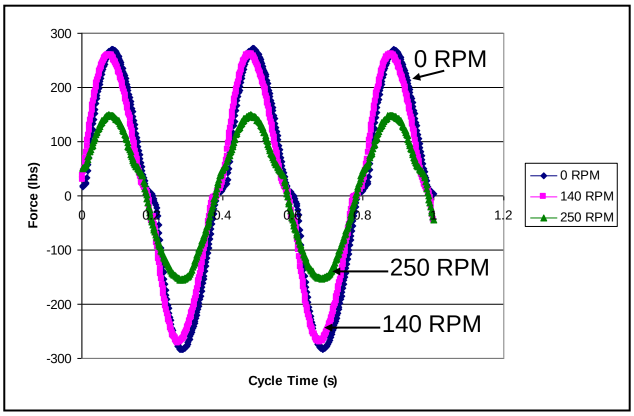

Figure 25: Force vs. Time of First Generation Damper in Spin Test Over Varying RPM

Figure 26 clearly shows that the bypass channels open at the desired rotor speed of 220 RPM, resulting in the nearly 50% reduction in damping at the forward flight rotor speed of 250 RPM.

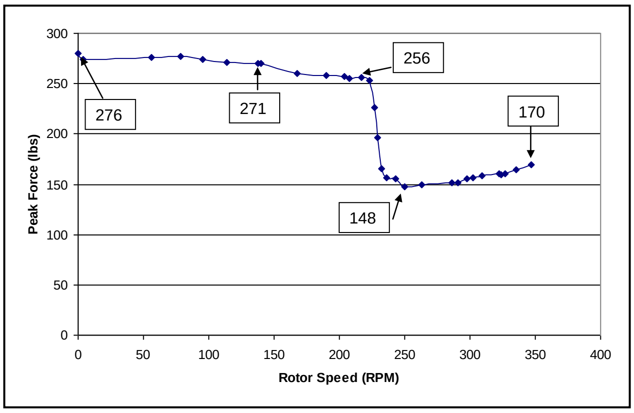

Figure 26: Damper Peak Force vs. Rotor RPM

5. CONCLUSIONS

A first and second generation multistate bypass lead-lag damper prototype were developed and bench tested, meeting the damping requirements for a generic light/medium helicopter in the closed configuration, and reducing forces in the open state. The first generation prototype was successfully spin tested, proving the CF actuation system in a representative environment. Additionally, the ability of computational fluid dynamics models to predict experimental damper behavior was compared. Some key conclusions of the testing are listed below:

1. The first generation prototype CF actuated multi-state damper, with three 0.4 inch diameter bypass channels, reduced damper forces by approximately 80% for the lead-lag condition of 2.5 Hz at 0.06 inches of dynamic displacement. Even larger reductions were achieved at higher frequencies and dynamic displacements.

2. The second generation prototype CF actuated multi-state damper with an integrated bypass orifice system demonstrated targeted 50% reductions in damping during bench tests.

3. The CFD model allowed for detailed investigation of flow behavior within the dampers. Comparison between predictions and experimental data showed errors well under 10% for most cases.

4. The first generation prototype was spin tested, proving the CF actuation system in a representative rotor environment.

5. Successful experimental bench testing, spin testing, and CFD predictions have verified the validity of the CF actuated multi-state bypass damper and proven the targeted adjustability of the damper behavior.

5.1 Future Work

Spin tests of the second generation prototype are currently being conducted. Upon completion, this technology will be ready to incorporate into new damper designs. LORD Corporation continues to pursue new damper technologies to enable further multi-state behavior.

ACKNOWLEDGMENTS

Special thanks to The Pennsylvania State University for their assistance in this research, and the use of the AERTS facility. We would also like to thank Dr. Jose Palacios for his support and coordination during the use of the AERTS facility.

REFERENCES

1 Kang, Hao, “Rotor Blade Lag Damping Using Embedded Chordwise Absorbers,” Ph.D. Dissertation, Department of Aerospace Engineering, Penn State University, State College, PA, 2001.

2 Byers, Lynn, “Helicopter Rotor Lag Damping Augmentation Using an Embedded Radial Vibration Absorber with Coriolis Coupling,” Ph.D. Dissertation, Department of Aerospace Engineering, Penn State University, State College, PA, May 2005.

3 McGuire, Dennis P., “Fluidlastic Dampers and Isolators for Vibration Control in Helicopters.” LORD Mechanical Products Division. Rept. LL-6502, Erie, PA, May 1994.

4 Brackbill, Christian R., “Helicopter Rotor Aeroelastic Analysis using a Refined Elastomeric Damper Model,” Ph.D. Dissertation, Department of Aerospace Engineering, Penn State University, State College, PA, 2000.

5 Cook, E., Hu, W., and Wereley, N. M., “Magnetorheological Bypass Damper Exploiting Flow Through a Porous Channel,” *Journal of Intelligent Material Systems and Structures,* Vol. 18*,* Sage Publications, 2007.

6 Reed, Donald A., “Lag Frequency Selective Damper.” Patent 3,638,885. 1 February 1972.

7 Bottasso, C. L., Cacciola, S., Croce, A., and Dozio, L. “Load Reduction in Lead-Lag Dampers by Speed-Scheduled Aperature and Modulated Control of a By-Pass Valve,” *Proceedings of the 66th Annual Forum of the AHS*, Phoenix, AZ, May 2010.

8 Wereley, N. M., and Pang, L., “Nondimensional Analysis of Semi-Active Electrorheological and Magnetorheological Dampers Using Approximate Parallel Plate Models,” *Smart Materials and Structures* Vol 7, IOP Publishing Ltd, UK, 1998.

9 Wereley, N. M., Lindler, J., Rosenfeld, N., and Choi, Y., “Biviscous Damper Behavior in Electrorheological Shock Absorbers,” *Smart Materials and Structures*, IOP Publishing LTD., UK, 2004.

10 Lindler, J., and Wereley, N. M., “Analysis and Testing of Electrorheological Bypass Dampers,” *Journal of Intelligent Material Systems and Structures*, Vol. 10, Technomic Pulblishing Co., Switzerland, 2000.

11 Gavin, H., “Muli-duct ER Dampers,” *Journal of Intelligent Material Systems and Structures*, Vol. 12, Sage Publications, 2001.

12 Yoo, J., and Wereley, N. M., “Design of a High-Efficiency Magnetorheological Valve,” *Journal of Intelligent Material Systems and Structures*, Vol. 13, Sage Publications, 2002.

13 Petrie, J., “Helicopter Rotor Blade Lag Damping Using Fluidlastic Embedded Chordwise Inertial Dampers,” MS Thesis, The Pennsylvania State University, August 2004.

14 Wang, S., “Transient Loads Control for a Stiff In-Plane Rotor Using an Embedded Device,” MS Thesis, The Pennsylvania State University, May 2010.

15 Tavner, A. C. R., Turner, J. D., and Hill, M., “A Rule-Based Technique for Two-State Switchable Suspension Dampers.” *Proceedings of the Institution of Mechanical Engineers*, Vol 211 Part D, Professional Engineering Publishing, UK, 1997.

16 American Helicopter Society paper “Multi-State Lead-Lag Damper Development and Validation” presented at the 67th Annual Forum, Virginia Beach, VA, May 3-5, 2011. Authored by:
Conor Marr, Research Assistant, Penn State
Zach Fuhrer, Sr. Engineer, LORD Corporation
George A. Lesieutre, Professor, Penn State
Edward C. Smith, Professor, Penn State